多田寛	樋口秀男、渡邊朋信、大内憲明	抗HER2抗体標識量子ドットを用いたマウス腫瘍内での単粒子イメージング	可視化情報	26	1	181	182	2006	
武田元博		医工連携のための技術者再教育プロジェクト	日本機械学会誌	109	1047	20	21	2006	
Watanabe T	Sato T, Gonda K, Higuchi H	Three-dimensional nanometry of vasicle transport in living cells using dual-focus imaging optics.	Biochem Biophys Res Commun	359		1	7	2007	
Mousavand T	Zhang J, Ohara S, Umetsu M, Naka T, Adschiri T	Organic-ligand-assisted supercritical hydrothermal synthesis of titanium oxide nanocrystals leading to perfectly dispersed titanium oxide nanoparticle in organic phase.	Journal of Nanoparticle Research	9		1067	1071	2007	
Lima R	Wada S, Takeda M, Tsubota K, Yamaguchi T	In vitro confocal micro-PIV measurements of blood flow in a square microchannel: The effect of the haematocrit on instantaneous velocity profi les.	Journal of Biomechanics	40		2752	2757	2007	○
Kobayashi Y	Imai J, Ngao D, Takeda M, Ohuchi N, Kasuya A, Konno M	Preparation of multilayered silica-Gd-silica core-shell particles and their magnetic resonance images.	Colloids and Surfaces A	308	1	14	19	2007	○
Kobayashi Y	Misawa K, Takeda M, Ohuchi N, Kasuya A, Konno M	Control of Shell Thickness in Silica-Coating of AgI Nanoparticles.	Advanced Materials Research	29-30		191	194	2007	○
Park YS	Kasuya A, Dmytruk A, Yasuto N, Takeda M, Ohuchi N, Sato Y, Tohji, K Uo M, Watari F	Concentrated colloids of silica-encapsulated gold nanoparticles: colloidal stability, cytotoxicity, and X-ray absorption.	J. Nanosci. Nanotec	7	8	2690	2695	2007	○

Park YS	Dmytruk A, Dmitruk I, Noda Y, Kasuya A, Takeda M, Ohuchi N	Aqueous-phase synthesis of ultra-stable small CdSe nanoparticles.	J. Nanosci. Nanotec	7	11	3750	3753	2007	○
Zhou X	Shao Z, Kobayashi Y, Wang X, Ohuchi N, Takeda M, Kasuya A	Photoluminescence of CdSe and CdSe/CdO·nH2O Core/Shell Nanoparticles Prepared in Aqueous Solution.	Optical Materials	29		1048	1054	2007	○
Kobayashi M	T. Mizumoto, T. Q. Duc, M. Takeda	Fluorescence Tomography of Biological Tissue Based on Ultrasound Tagging Technique	Proc. SPIE	6633		663306-1-5		2007	○
Kobayashi M	K Sasaki, M Enomoto, Y. Ehara	Highly sensitive determination of transient generation of biophotons during hypersensitive response to cucumber mosaic virus in cowpea.	J. Exp. Botany	58	3	465	472	2007	
Park YS	Kasuya A, Dmytruk A, Yasuto N, Takeda M, Ohuchi N, Sato Y, Tohji K, Uo M, Watari F	Concentrated colloids of silica-encapsulated gold nanoparticles: colloidal stability, cytotoxicity, and X-ray absorption.	J. Nanosci. Nanotec	7	8	2690	2695	2007	○
Dmytruk A	Park YS, Kasuya A, Kikuchi H, Takahashi M, Kawazoe Y, Watanabe A	Silicon subiodide clusters.	J. Nanosci. Nanotec	7	11	3788	3791	2007	○
Takahashi N	Gombojav B, Yoshinari T, Takahashi Y, Nagasaka S, Yamamoto A, Goto T, Kasuya A	Luminescences of Pyrene Single Crsytal and Pyrene Molecules Inserted in a Molecular Vessel of Cyclodextrin	J. Phys. Soc. Japan	76		34703	34705	2007	
武田元博	武田元博、小林芳男、小林正樹、桜井遊、権田幸祐、樋口秀男、大内憲明	機能性ナノ粒子による生体イメージングの医療展開	ナノ学会誌	6	2	49	56	2008	○
Lima R	Wada S, Tanaka S, Takeda M, Ishikawa T, Tsubota K, Imai Y, Yamaguchi T	In vitro blood flow in a rectangular PDMS microchannel: experimental observations using a confocal micro-PIV system.	Biomecd Microdevices	10	2	153	167	2008	○

Kobayashi Y	Shimizu N, Misawa K, Takeda M, Ohuchi N, Kasuya A, Konno M	Preparation of amine free silica coated AgI nanoparticles with modified Stöber method.	Surfaces Engineering	24	4	248	252	2008	○
Romanyuk V	Dmitruk I, Barnakovl Yu, Belosludov R, Kasuya A	Ultra-Stable Nanoparticles in AIIBVI (AII = Cd, Zn; BVI = S, Se, Te)	Compounds Journal of Nanosci. and Nanotech	8		1	8	2008	○
Kandori T	Hayase T, Inoue K, Funamoto K, Takeno T, Ohta M, Takeda M, Shirai A	Frictional Characteristics of Erythrocytes on Coated Glass Plates Subject to Inclined Centrifugal Forces.	Journal of Biomedical Engineering	130	5	51007-1	51007-8	2008	○
Takeda M	Tada H, Higuchi H, Kobayashi Y, Kobayashi M, Sakurai Y, Ishida T, Ohuchi N	In vivo single molecular imaging and sentinel node navigation by nano-technology for molecular targeting drug delivery system and tailor made medicine.	Breast Cancer	15	2	145	152	2008	○
Kohno M	Takeda M, Niwano Y, Saito R, Emoto N, Tada M, Kanazawa T, Ohuchi N, Yamada R	Early diagnosis of cancer by detecting the chemiluminescence of hematoporphyrins in peripheral blood lymphocytes	Tohoku J. Exp. Med.	216	1	47	52	2008	○
Suvitha A	Belosludov RV, Mizuseki H, Kawaoe Y, Takeda M, Kohno K, Ohuchi N	TD-DFT studies on hematoporphyrin and its dimers	Materials Transactions	49	11	2416	2419	2008	○
Yoo J	Kambara T, Gonda K, HiguchiH	Intracellular imaging of targeted proteins labeled with Quantum Dots.	Experimental Cell Research	314	19	3563	3569	2008	○
武田元博	権田幸祐、樋口秀男、大内憲明	がん分子イメージングの新展開	癌と化学療法	35	8	1277	1280	2008	○
武田元博	桜井　遊、叢　莉蔓、小林芳男、菅原旭浩、大内憲明	新規開発ナノサイズヨウ化銀ビーズを用いたＸ線ＣＴ造影効果および体内動態の検討	乳癌基礎研究	17		57	60	2008	
小林正樹		生命科学・医学応用のための極微弱発光・蛍光イメージング技術	顕微鏡	43	3	202	206	2008	

Dmytruk A	Dmitruk I, Blonsky I, Belosludov R, Kawazoe Y, Kasuya A	ZnO clusters: Laser ablation production and time-of-flight mass spectroscopic study	Microelectronics J	40		218	220	2009	○
Ishida T	Kiba T, Motohiro Takeda M, Matsuyama K, Satoshi Teramukai S, Ishiwata R, Masuda N, Yuichi Takatsuka Y, Noguchi S, Ishioka C, Fukushima M, Ohuchi N	Phase II study of capecitabine and trastuzumab combination chemotherapy in patients with HER2 overexpressing metastatic breast cancers resistant to both anthracyclines and taxanes	Cancer Chemother Pharmacol					in press	○

別紙２

書籍　(2006ー2008年)

著者氏名	連名著者氏名	編集者名	論文タイトル名	書籍名	出版社名	出版地	出版年	開始頁	終了頁
大内憲明	武田元博、石田孝宣	山田章吾	手術と放射線	早期のがん治療法の選択　放射線治療	金原出版	東京	2006	46	51
佐々木隆史	名嘉節、大原智、阿尻雅文	山本重夫	蛍光特性ナノ粒子の表面修飾	量子ドットの生命科学領域への応用	シーエムシー出版社	東京	2007	115	121
武田元博	小林芳男、小林正樹、桜井遊、甘利正和、石田孝宣、鈴木昭彦、大内憲明	宇理須恒雄	機能性ナノ粒子による生体イメージング―がん診療への応用―	ナノメディシン ナノテクノ医療応用	オーム社	東京	2008	64	74
樋口秀男	大内憲明	宇理須恒雄	単一量子ドットのバイオ・医療ナノイメージング	ナノメディシン ナノテクノ医療応用	オーム社	東京	2008	52	63
武田元博	権田幸祐、大内憲明	川口春馬	機能性ナノ粒子の医学領域における展開	有機分散系の分散・凝集技術	シーエムシー出版	東京	2008	252	261
大原　智	梅津光央，名嘉　節，高見誠一，阿尻雅文	佐古 猛	超臨界水を用いたナノ粒子製造	超臨界流体技術の開発と応用	シーエムシー出版	東京	2008	56	61

別紙３

学会発表　(2006～2008)

国内

平成18年東北地区若手研究者研究発表会、2006/2/28、仙台
伊藤勇樹、今野淳、鈴木聡、武田元博、小林正樹
培養がん細胞由来バイオフォトンの検出と代謝活性計測への応用

菊地大輔、青山史裕、泉谷一也、岡村均、小林正樹
超高感度CCDを用いたヒト体表バイオフォトンイメージングによる生理情報計測Ⅰ－生体リズムとバイオフォトン発光－

青山史裕、菊地大輔、泉谷一也、小林正樹
超高感度CCDを用いたヒト体表バイオフォトンイメージングによる生理情報計測Ⅱ－バイオフォトン発光の体表温度依存性－

水本憲、渋谷幸弘、児玉優、榎本幹、小林正樹
超音波－光相互作用に基づく生体内蛍光イメージング法の基礎検討

第45回日本生体医工学会大会、2006/5/15-17、福岡
水本憲、渋谷幸弘、榎本幹、武田元博、小林正樹
集束超音波を用いた超音波－光相互作用に基づく散乱媒質内蛍光イメージング法の基礎検討

今野淳、鈴木聡、武田元博、水野麻弥、小川雄一、川瀬晃道、小林正樹
培養がん細胞AH109からのバイオフォトン検出による細胞代謝活性計測の検討

平成18年度電気関係学会東北支部連合大会、2006/8/31-9/1、秋田
水本憲、武田元博、榎本幹、小林正樹
超音波－光相互作用を利用した生体蛍光断層画像計測法の基礎検討

菊地大輔、岡村均、小林正樹
ヒト体表バイオフォトン画像計測によるバイオフォトン発光と生体リズムの相関の検討

第27回日本レーザー医学会総会、2006/11/2-3、東京
水本憲、武田元博、榎本幹、小林正樹
超音波－光相互作用を利用した生体蛍光断層画像計測法の基礎検討

菊地大輔、岡村均、小林正樹
超高感度ＣＣＤによるヒト体表バイオフォトン概日リズムの画像計測

第40回日本生体医工学会東北支部大会、2006/11/25、仙台
水本憲、武田元博、榎本幹、小林正樹
超音波－光相互作用を利用した生体蛍光断層画像計測法の基礎検討

菊地大輔、岡村均、小林正樹
超高感度バイオフォトンイメージングによるヒト体表バイオフォトンのサーカディアンリズム分析

第61回応用物理学会東北支部学術講演会、2006/12/7-8、仙台
水本憲、武田元博、榎本幹、小林正樹
音響光学効果を利用した生体計測のための超音波タグ蛍光イメージング法

第8回化学工学会学生発表会、2006/3/11、一関
清水直樹、小林芳男、武田元博、大内憲明、今野幹男
X線造影用AgI/Si02コアーシェル型複合粒子の合成

第106回日本外科学会定期学術集会、2006/3/29-31、東京
桜井　遊、武田元博、小林芳男、中島護雄、亀井　尚、粕谷厚生、川添良幸、大内憲明
新規ナノサイズヨウ化銀ビーズを用いた造影効果と体内動態の検討

中島護雄、武田元博,大内憲明
蛍光ビーズを用いたセンチネルリンパ節生検法の検討

武田元博、大内憲明
ガドリニウムナノ粒子を用いた新規MRI造影剤の基礎的検討

第14回日本乳癌学会総会、2006/7/7-8、金沢
桜井　遊 、武田元博、小林芳男、中島護雄、亀井　尚、粕谷厚生、川添良幸、大内憲明

桜井　遊 、武田元博、小林芳男、中島護雄、亀井　尚、柏谷厚生、川添良幸、大内憲明
新規ナノサイズヨウ化銀ビーズを用いたセンチネルリンパ節の造影 効果と体内動態の検討

多田寛、樋口秀男、渡邉朋信、大内憲明
Quantum dotを用いたHER2発現乳癌担癌マウス腫瘍内での蛍光単粒子イメージング

2007年生体運動合同班会議、2007/1/7-9、金沢
権田幸祐、渡辺朋信、樋口秀男
量子ドットを用いたマウス腫瘍内細胞運動のイメージング

第56回日本癌学会総会、2006/9/29-31、横浜
樋口秀男、渡邉朋信、多田寛、大内憲明
機能性ナノ粒子を用いたがん細胞の単一粒子ナノイメージング

第61回日本体力医学会、2006/9/24-26、神戸
樋口秀男、渡邉朋信、多田寛、大内憲明
光学顕微鏡技術を用いた、タンパク質・細胞・マウス内単一分子のイメージング

ナノ学会第４回大会、2006/5/19-21、京都
何合賢朗、樋口秀男、渡辺朋信、多田寛、大内憲明
抗EGFR抗体標識量子ドットを用いたヒト乳癌細胞のマウスin vivoイメージング

第34回可視化情報シンポジウム、2006/7/24-26、東京
多田寛、樋口秀男、渡邉朋信、大内憲明
抗HER2抗体標識量子ドットを用いたマウス腫瘍内での単粒子イメージング

第15 回日本バイオイメージング学会、2006/10/31/-11/2、盛岡
樋口秀男、渡辺朋信、権田幸祐
細胞およびマウス内の1 分子ナノイメージング

日本分子生物学会2006フォーラム、2006/12/6-8、名古屋
権田幸祐、渡辺朋信、樋口秀男
マウス腫瘍内の細胞運動の解析

第65回日本癌学会学術総会、2006/9/28-30、横浜
樋口秀男、渡邉朋信、多田寛、大内憲明
機能性ナノ粒子を用いたがん細胞の単一粒子ナノイメージング

武田元博、中島護雄、小林芳男、小林正樹、桜井遊、亀井尚、麗莉蔓、甘利正和、柏谷厚生、石田孝宣、鈴木昭彦、大内憲明
機能性ナノ粒子を用いたセンチネルリンパ節イメージング

2008年春季第55回応用物理学関係連合講演会
異分野融合ナノテクノロジー横浜コロキウム、平成20年2月1日、横浜
武田元博、樋口秀男、大内憲明
機能性ナノ粒子の医学領域における展開

第１７回乳癌基礎研究会、平成19年7月28-29日、大阪
武田元博、桜井遊、小林芳男、麗莉蔓、甘利正和、亀井尚、石田孝宣、鈴木昭彦、菅原旭浩、大内憲明
ナノサイズヨウ化銀ビーズの腫瘍とセンチネルリンパ節のX線CT造影効果

第66回日本癌学会学術総会、2007年10月、横浜
Takeda M, Higuchi H and Ohuchi N
Nano-imaging of single quantum dots and nano-particles in mice tumor.

第66回日本癌学会学術総会、2007年10月、横浜
Kawai M, Higuchi H, Takeda M and Ohuchi N
In Vivo Imaging of Vascular Permeability Using Nanocrystals in Mice Tumor.

ナノ学会第5回大会、2007年5月、つくば市
何合賢朗、樋口秀男、大内憲明
マウス腫瘍新生血管における透過性のIn vivo imaging.

第107回日本外科学会総会、2007年4月、大阪
甘利　正和、石田　孝宣、武田　元博、鈴木　昭彦、宇佐見　伸、多田　寛、大内　憲明
進行・再発乳癌におけるカペシタビンの治療効果の検討

第15回日本乳癌学会学術総会、2007年6月、横浜
甘利正和、石田孝宣、武田元博、鈴木昭彦、大内憲明
若年者乳癌の臨床病理学的検討

第15回日本乳癌学会総会、2007年6月、横浜
大内憲明、多田寛、河合賢朗、武田元博、石田孝宣、樋口秀男
生体超微細1分子可視化によるナノDDSと乳癌標的治療

平成19年東北地区若手研究者研究発表会、講演番号YS-5-50、講演資料p. 79 (2007)
大原健、鈴木祐輔、水本衛、榎本幹、武田元博、小林正樹
超音波タグ蛍光イメージング法による生体試料の蛍光断層計測

平成19年東北地区若手研究者研究発表会、講演番号YS-5-08、講演資料p. 15 (2007)
山内崇弘、渡邉尚哉、小林正樹
超高感度CCDを用いたヒト生物フォトンイメージングによる皮膚酸化ストレス計測の検討

平成19年東北地区若手研究者研究発表会、講演番号YS-5-09、講演資料p. 17 (2007)
菊地大輔、千葉朋子、小林正樹
極微弱発光による化学反応波の動態計測とイメージング

平成19年東北地区若手研究者研究発表会、講演番号YS-5-10、講演資料p. 19 (2007)
熊坂増高、内堀綾斗、武田元博、亀井尚、桜井遊、大内憲明、小林正樹
がん転移診断のためのセンチネルリンパ節蛍光イメージング法の検討－ブタを用いた腹腔内視鏡による観察－

第55回日本臨床検査医学会　学術集会、シンポジウム10：医学領域におけるナノ粒子展開をめぐる話題「機能性ナノ粒子による生体イメージングの臨床検査への応用」　2008年11月27－30日、名古屋
武田元博、権田幸祐、桜井 遊、河合賢朗、石田孝宣、大内憲明
機能性ナノ粒子による生体イメージングの臨床検査・外科への応用

2008年（平成20年）春季応用物理学関係連合講演会　ナノテクの難病研究・医療への応用、2008年3月27－30日、千葉
武田元博、樋口秀男、小林正樹、小林芳男、大内憲明
機能性ナノ粒子によるナノからマクロレベルの生体イメージング

第31回日本分子生物学会・第81回日本生化学会合同大会、神戸、2008年12月
権田幸祐、渡邉朋信、武田元博、樋口秀男、大内憲明
In vivoイメージングで観えてきた癌転移の仕組み

2009年生体運動合同班会議、東京大学、2009/01/09-10
権田幸祐、渡邉朋信、武田元博、大内憲明、樋口秀男
がん細胞の膜のダイナミックスは転移の進行にともない劇的に変化する

化学工学会第73年会 平成20年3月17－19日、浜松
倉真理絵、小林芳男、武田元博、粕谷厚生、大内憲明
AgI/SiO2複合粒子コロイドの調製法の開発

第１８回乳癌基礎研究会、平成20年7月12-13日、福島
河合賢朗、武田元博、石田孝宣、大内憲明
粒径の異なるナノ粒子による腫瘍間質ドラッグデリバリーシステムの解析

第125回バイオメカニクス研究会（日本生体医工学会専門別研究会）、(東北大) 2008年 10月
権田幸祐、武田元博、樋口秀男、大内憲明
In vivoナノイメージングで観えてきた癌転移の仕組み

ナノ学会第６回大会、福岡、2008/05/07-09
権田幸祐、渡邉朋信、武田元博、大内憲明、樋口秀男
量子ドットを用いた腫瘍細胞の膜伸縮運動のin vivoイメージング

ナノ学会第６回大会、福岡、2008/05/07-09
義利憂、小林芳男、武田元博、櫻井遊、甘利正和、大内憲明
シリカコーティング蛍光ナノビーズによるセンチネルリンパ節生検と分子画像診断

ナノ学会第６回大会、福岡、2008/05/07-09
武田元博、小林芳男、小林正樹、桜井遊、権田幸祐、樋口秀男、大内憲明
ナノヨウ化銀ビーズによるCT造影法の外科応用に関する基礎的検討

ナノ学会第６回大会，福岡，2008/05/07-09（若手優秀発表賞受賞）
河合賢朗，武田元博，石田孝宣，大内憲明
蛍光ナノ粒子を用いた担がんマウスにおける腫瘍間質ナノドラッグデリバリーシステムの解析

ナノ学会第６回大会，福岡，2008/05/07-09
日景充，亀井尚，武田元博，小林正樹，大内憲明
新規ナノ粒子をトレーサーとした鏡視下手術の基礎的検討

第108回日本外科学会定期学術集会，長崎，2008/05/15-17
河合賢朗，樋口秀男，武田元博，石田孝宣，鈴木昭彦，甘利正和，宇佐美伸，桜井遊，渡部剛，大内憲明
腫瘍間質におけるナノスケールでの分子挙動解析によるDDSの解明

異分野融合ナノテクノロジー横浜コロキウム，平成20年2月1日，横浜
武田元博，樋口秀男，大内憲明
機能性ナノ粒子の医学領域における展開

第１８回乳癌基礎研究会，平成20年7月12-13日，福島
武田元博，阿野雅弘，佐藤恵美子，山田理恵，甘利正和，鈴木昭彦，石田孝宣，大内憲明
ヘマトポルフィリン誘導体計測によるがん診断の基礎的検討

平成20年年度電気関係学会東北支部連合大会，講演番号2E14，講演論文集p．183（2008）
南部雄也，鈴木知佳，高橋誠樹，Trinh Quang Duc，小林正樹
超音波タグ蛍光断層イメージング法による生体組織の蛍光断層画像計測

平成20年年度電気関係学会東北支部連合大会，講演番号2E15，講演論文集p．184（2008）
熊坂増高，日景充，亀井尚，武田元博，大内憲明，小林正樹
ナノ蛍光微粒子によるセンチネルリンパ節検索のための腹腔内視鏡蛍光イメージングシステムの開発

第６０回日本細胞生物学会　ワークショップ（パシフィコ横浜）2008年 7月
権田幸祐，渡邉朋信，武田元博，大内憲明，樋口秀男
量子ドットを用いた腫瘍細胞のin vivoイメージング

第61回コロイドおよび界面化学討論会平成20年9月
神真理絵，小林芳男，武田元博，粕谷厚生，大内憲明
医療検査用コア・シェル型複合粒子の合成に関する研究

国際（海外）

Li-Shishido S, Watanabe T, Tada H, Kawai M, Higuchi H, Ohuchi N.
Reduction in nonfluorescence state of quantum dots on an immunofluorescence staining.
The 9th International Symposium of Future Medical Engineering based on Bio-manotechnology, January 7-9, 2007, Sendai.

Tada H, Higuchi H, Watanabe T, Ohuchi N.
In vivo imaging using quantum dots in mice.
The 9th International Symposium of Future Medical Engineering based on Bio-manotechnology, January 7-9, 2007, Sendai.

Sakurai Y, Takeda M, Kasuya A, Kobayashi Y, Kamei I, Amari M, Cong L, Ohuchi N.
Nano size silver iodide beads as novel contrast media for sentinel lymph node navigation surgery.
The 9th International Symposium of Future Medical Engineering based on Bio-manotechnology, January 7-9, 2007, Sendai.

Sasaki T, Ohara S, Umetsu M, Naka T, Adschiri T
Supercritical Hydrothermal Synthesis of Hybrid Gd(OH)3 Nanoparticles : Application to Neutron Capture Therapy
The 1st international symposium on supercritical fluid synthsis and materials, Mar.2007, Beijing, China.

Kawai M, Higuchi H, Ohuchi N.
Trastuzumab regulates receptor recycling on cancer cell.
The 9th International Symposium of Future Medical Engineering based on Bio-manotechnology, January 7-9, 2007, Sendai.

Cong L, Takeda M, Ohuchi N.
Silica coated nano-particles for biomedical contrast imaging.
The 9th International Symposium of Future Medical Engineering based on Bio-manotechnology, January 7-9, 2007, Sendai.

Li-Shishido S, Watanabe T, Tada H, Kawai M, Higuchi H, Ohuchi N.
Reduction in nonfluorescence state of quantum dots on an immunofluorescence staining.
The 9th International Symposium of Future Medical Engineering based on Bio-manotechnology, January 7-9, 2007, Sendai.

Tada H, Higuchi H, Watanabe T, Ohuchi N.
In vivo imaging using quantum dots in mice.
The 9th International Symposium of Future Medical Engineering based on Bio-manotechnology, January 7-9, 2007, Sendai.

Sakurai Y, Takeda M, Kasuya A, Kobayashi Y, Kamei t, Amari M, Cong L, Ohuchi N.
Nano size silver iodide beads as novel contrast media for sentinel lymph node navigation surgery.
The 9th International Symposium of Future Medical Engineering based on Bio-manotechnology, January 7-9, 2007, Sendai.

Takeda M, Tada H, Kawai M, Sakurai Y, Higuchi H, Ohuchi N,
In vivo Single Molecular Imaging and Sentinel Node Navigation using Nano-biotechnology for Medical Application.
The 3rd Tohoku-NUS Symposium on Nano-Biomedical Engineering in the East Asian-Pacific Rim Region, 10-11 Dec 2007, National University of Singapore.

Kawai M, Takeda M, Higuchi H, Ohuchi N,
Tumor Interstitial Nano-particle Delivery and Analysis in the Human Tumor Xenograft in Mice.
The 3rd Tohoku-NUS Symposium on Nano-Biomedical Engineering in the East Asian-Pacific Rim Region, 10-11 Dec 2007, National University of Singapore.

Hamanaka Y, Takeda M, Tada H, Kawai M, Sakurai Y, Amari M, Suzuki A, Ishida T, Ohuchi N,
In vivo tracking of anti-cancer drugs and the active sites conjugated with quantum dots.
The 3rd Tohoku-NUS Symposium on Nano-Biomedical Engineering in the East Asian-Pacific Rim Region, 10-11 Dec 2007, National University of Singapore.

Sakurai Y, Takeda M, Cong L, Amari M, Kasuya A, Kobayashi Y, Kamei T, Ohuchi N,
In vivo Distribution of Silver Iodide Beads in Cancerous Legions.
The 3rd Tohoku-NUS Symposium on Nano-Biomedical Engineering in the East Asian-Pacific Rim Region, 10-11 Dec 2007, National University of Singapore.

Duc TQ, Mizumoto T, Nanbu Y, Takeda M, Kobayashi M,
Tomographic Imaging of Fluorophore Embedded in Biological Tissue Based on Ultrasound Tagging Technique.
The 7th pacific Rim Conference on Lasers and Electro-Optics (CLEO), Abstract pp.1193-1194, August, 2007, Seoul, Korea.

Kawai, M., Higuchi, H., Gonda, K., Takeda, M., and Ohuchi, N.
In vivo imaging of vascular permeability using nano-objects in mice tumor.
2nd "Hot Topics in Molecular Imaging - TOPIM" meeting of the European Society for Molecular Imaging. February 2008, Grenoble, France.

Ohuchi, N., Takeda, M., Kawai, M., Tada, H. Sakurai, Y., Gonda, K., and Higuchi, H.
Novel imaging techniques with functional nano-objects for cancer diagnosis.
2nd "Hot Topics in Molecular Imaging - TOPIM" meeting of the European Society for Molecular Imaging. February 2008, Grenoble, France.

Ohuchi N, Takeda M, Kawai M, Tada H, Sakurai Y, Gonda K, Higuchi H.
Novel imaging techniques with functional nano-objects for cancer diagnosis
Hot Topics in Molecular Imaging 2008 (TOPIM'08), Eiropean Society for Molecular Imaging, February 4-8, 2008, Les Houches, France.

Kawai M, Higuchi H, Gonda K, Takeda M, Ohuchi N.
In vivo imaging of vascular permeability using nano-objects in mice tumor.
Hot Topics in Molecular Imaging 2008 (TOPIM'08), Eiropean Society for Molecular Imaging, February 4-8, 2008, Les Houches, France.

Ohuchi N, Takeda M, Kawai M, Tada H, Sakurai Y, Gonda K, Higuchi H.
Molecular imaging with functional nano-objects for cancer diagnosis.
The 5th International Symposium on Nano-Biomedical Engineering Education and Research Centre. March, 27-28, 2008, Matsushima, Japan

Ishida T, Kiba T, Takeda M, Matsuyama K, Teramukai S, Masuda N, Takatsuka Y, Noguchi S, Fukushima M, Ohuchi N.
Phase II study of Capecitabine and Trastuzumab combination chemotherapy in patients with HER2 overexpressing metastatic breast cancers after failure of both Anthracyclines and Taxanes.
The 44th American Society of Clinical Oncology (ASCO) Annual Meeting, May 30 - June 3, 2008, Chicago

Suzuki T, Moriya T, Hayashi S, Ohuchi N, Sasano H.
Intratumoral concentration of sex stereoids in ductal carcinoma in situ (DCIS) of human breast. Breast Cancer, 15, Supplement 1, 10-10, 2008
The 26th Congress of the International Association for Breast Cancer Research, September 22-24, 2008, Kurashiki, Japan

Nakano T, Tse GM, Tan PH, Kozuka Y, Kanomata N, Ishida T, Ishida K, Watanabe M, Tamaki K, Ohuchi N, Sasano H, Moriya T.
Triple negative subtype of ductal carcinoma in situ in Asian women. Breast Cancer, 15, Supplement 1, 19-19, 2008
The 26th Congress of the International Association for Breast Cancer Research, September 22-24, 2008, Kurashiki, Japan

Kozuka Y, Moriya T, Akiyama F, Kurosumi M, Tse GM, Tan PH, Kanomata N, Ohuchi N, Kurebayashi J, Sasano H.
Breast Cancer, 15, Supplement 1, 19-20, 2008
The 26th Congress of the International Association for Breast Cancer Research, September 22-24, 2008, Kurashiki, Japan

Kawai M, Takeda m, Ishida T, Suzuki A, amari M, Ohuchi N.
Breast Cancer, 15, Supplement 1, 33-33, 2008
The 26th Congress of the International Association for Breast Cancer Research, September 22-24, 2008, Kurashiki, Japan

Takeda M, Sakurai Y, Kobayashi Y, Cong L, Hikage M, Amari M, Ishida T, Gonda K, Ohuchi N.
Breast Cancer, 15, Supplement 1, 37-37, 2008
The 26th Congress of the International Association for Breast Cancer Research, September 22-24, 2008, Kurashiki, Japan

Harada N, Yamada T, Ishida T, Takeda Suzuki A, Amari M, Moriya T, Ohuchi N.
Breast Cancer, 15, Supplement 1, 36-36, 2008
The 26th Congress of the International Association for Breast Cancer Research, September 22-24, 2008, Kurashiki, Japan.

Gonda, K., Takeda, M., Kawai, M., Sakurai Y, Higuchi H., Ohuchi, N.
Imaging of cancer metastasis in living tumor with quantum dots.
The 7th International Symposium on Nano-Biomedical Engineering, October 2008, National Cheng Kung University, Tainan.

Takeda M, Tada H, Kawai, M, Sakurai Y, Cong L, Gonda K, Higuchi H, Ohuchi N.
Bio-imaging by functional nano-particles of nano to macro scale.
The 13th International Conferencenon Biomedical Engineering, December 3-6.2008, Singapore.

Kawai, M, Takeda M, Ohuchi N.
The feature of the interstitial nano drug delivery system with fluorescent nanocrystals of different sizes in the human tumor xenograft in mice.
The 13th International Conferencenon Biomedical Engineering, December 3-6.2008, Singapore.

Cong L, Takeda M, Watanabe M, Kobayashi Y, Kobayashi M, Ohuchi N.
Silica-coated fuorescent nano-Particles for sentinel lymph node biopsy and mapping.
Tohoku-NUS student joint symposium. December 9-10, 2008, Singapore.

Gonda K, Watanabe TM, Takeda M, Higuchi H and Ohuchi N.
In vivo imaging of membrane dynamics in metastatic tumor cells.
The 2nd International Symposium on Nanomedicine, Asian Core Symposium-Nano and Biomedical Molecular Science-, February 4-7, 2009, Okazaki, Japan.

Duc TQ, Y. Nanbu, T. Suzuki, S. Takahashi, M. Takeda, M. Kobayashi M.
Basic study on application of the phased-array transducer to determine fluorescence in turbid media based-on acousto-optic effects.
International Conference on Laser Applications in Life Sciences (LALS 2008), Abstract book p. 7, December 4 2008, Taipei, Taiwan.

Duc TQ, Y. Nanbu, T. Suzuki, S. Takahashi, M. Takeda, M. Kobayashi M.
Fluorescence tomography based-on acousto-optic modulations with phased-array ultrasound transducer.
BiOS Part of SPIE Photonic West, paper No. 7177-57, January 27, 2009, San Jose, USA.

別紙4

特許財産権の出願登録状況　(2006ー2007年)

内容	発明者	権利者	知的財産権の種類	番号	出願年月日	取得年月日
蛍光断層画像計測装置	小林正樹,(株)システム計測	小林正樹	特許	特開2006-055396	2004年8月20日	
がん細胞運動およびがん細胞浸潤抑制剤	権田幸祐、樋口秀男	東北大学	特許	特願2008ー083588	2008年3月27日	

新聞記事

誌名	年月日	タイトル
河北新報	2007.2.8	抗がん剤動き把握　分子レベル画像化

Ⅳ. 研究成果の刊行物・別刷

Research Article

In vivo Real-time Tracking of Single Quantum Dots Conjugated with Monoclonal Anti-HER2 Antibody in Tumors of Mice

Hiroshi Tada,[1] Hideo Higuchi,[2] Tomonobu M. Wanatabe,[2] and Noriaki Ohuchi[1]

[1]Division of Surgical Oncology, Graduate School of Medicine and [2]Biomedical Engineering Research, Organization, Tohoku University, Sendai, Japan

Abstract

Studies with tracking of single nanoparticles are providing new insights into the interactions and processes involved in the transport of drug carriers in living mice. Here, we report the tracking of a single particle quantum dot (Qdot) conjugated with tumor-targeting antibody in tumors of living mice using a dorsal skinfold chamber and a high-speed confocal microscope with a high-sensitivity camera. Qdot labeled with the monoclonal anti-HER2 antibody was injected into mice with HER2-overexpressing breast cancer to analyze the molecular processes of its mechanistic delivery to the tumor. Movement of single complexes of the Qdot-antibody could be clearly observed at 30 frames/s inside the tumor through a dorsal skinfold chamber. We successfully identified six processes of delivery: initially in the circulation within a blood vessel, during extravasation, in the extracelullar region, binding to HER2 on the cell membrane, moving from the cell membrane to the perinuclear region, and in the perinuclear region. The six processes were quantitatively analyzed to understand the rate-limiting constraints on Qdot-antibody delivery. The movement of the complexes at each stage was "stop-and-go." The image analysis of the delivery processes of single particles *in vivo* provides valuable information on antibody-conjugated therapeutic nanoparticles, which will be useful in increasing therapeutic efficacy. [Cancer Res 2007;67(3):1–7]

Introduction

Recent anticancer therapeutics based on active tumor targeting by conjugating tumor-specific antibodies has become of great interest in oncology, pharmacology, and nanomedicine. This approach will allow to increase therapeutic efficacy and to decrease systemic toxicity (1–3). Quantitative investigation of the dynamics of such delivery *in vivo* is crucial in enabling the development of more effective drug delivery systems. One of the best ways to do this is to apply a new technology in biophysics wherein the positions of proteins are detected quantitatively at the single molecule or particle level with nanometer precision (4). However, the specific processes of its delivery *in vivo* postinjection are not known at the single particle level. Conventional modalities of *in vivo* imaging such as computed tomography, magnetic resonance imaging, positron emission tomography, and organic fluorescence or luminescence imaging have insufficient resolution to analyze the pharmacokinetics of drugs at the single particle level *in vivo* (5).

To address the issue, real-time single particle tracking using quantum dots (Qdots) has been applied to the study of drug delivery. Qdots, fluorescence nanocrystals, were thought to be as a suitable marker because of their intense brightness and stability, in contrast to organic dyes and green fluorescent protein (6–8). In cultured cells, single particle tracking has yielded invaluable information on the function of purified proteins (9–11). Recent work shows that the antibody-conjugated Qdots have allowed real-time tracking of single receptor molecules on the surface of live cells (12). However, no real-time single particle tracking in live animals has been reported, and it is uncertain that single particles of Qdots could be observed and tracked in live animals. The analysis of single molecules and particles in living animals is crucial to the understanding of the molecular mechanism of proteins *in vivo*.

This study was designed to analyze the movement of single functional Qdots in tumors of mice from a capillary vessel to cancer cells. To observe single Qdot particles in tumor tissue, we used a dorsal skinfold chamber model (13) and a high-resolution intravital imaging system. The imaging system, which consists of a confocal scanner unit with a Nipkow type disk and an electron multiplying charge coupled device (EMCCD) camera (14), facilitates the high-resolution *in vivo* single particle tracking at a video rate with a high spatial resolution of 30 nm. In addition, quantitative and qualitative information such as velocity, directionality, and transport mode was obtained using time-resolved trajectories of particles. As a result, we successfully identified the processes of delivery; these were quantitatively analyzed to understand the rate-limiting constraints on single Qdot-antibody delivery *in vivo*.

Materials and Methods

Qdot-antibody conjugation. Qdot was conjugated to trastuzumab (Herceptin, Chugai Pharmaceuticals Co., Ltd., Tokyo, Japan) with a Qdot 800 Antibody Conjugation Kit (Quantum Dot Corp., Hayward, CA) coated with polyethylene glycol (PEG) amine (MW 2,000) according to the manufacturer's instruction. Briefly, Qdots are activated with the heterobifunctional cross-linker 4-(maleimidomethyl)-1-cyclohexanecarboxylic acid *N*-hydroxysuccinimide ester (SMCC), yielding a maleimide-nanocrystal surface. Excess SMCC is removed by size exclusion chromatography. Antibody is then reduced and fragmented by DTT to expose free sulfhydryls, and excess DTT is removed by size exclusion chromatography. Then, activated Qdots are covalently coupled with reduced antibody and reaction is quenched with β-mercaptoethanol. The molar ratio of trastuzumab fragments to the Qdots at mixing is ~3:1. Conjugates are concentrated by ultrafiltration and purified by size exclusion chromatography. This active ester maleimide-mediated amine and sulfhydryl coupling (by SMCC) is a popular cross-linking reaction for various antibody conjugations. After this reduction, it

Note: Supplementary data for this article are available at Cancer Research Online (http://cancerres.aacrjournals.org/).

Requests for reprints: Hideo Higuchi, Biomedical Engineering Research Organization, Tohoku University, Engineering research Lab complex, 6-6-11 Aramaki, Aoba-ku, Sendai, Miyagi 980-8578, Japan. Phone: 81-22-795-4735; Fax: 81-22-795-5753; E-mail: higuchi@tubero.tohoku.ac.jp.

doi:10.1158/0008-5472.CAN-06-1185

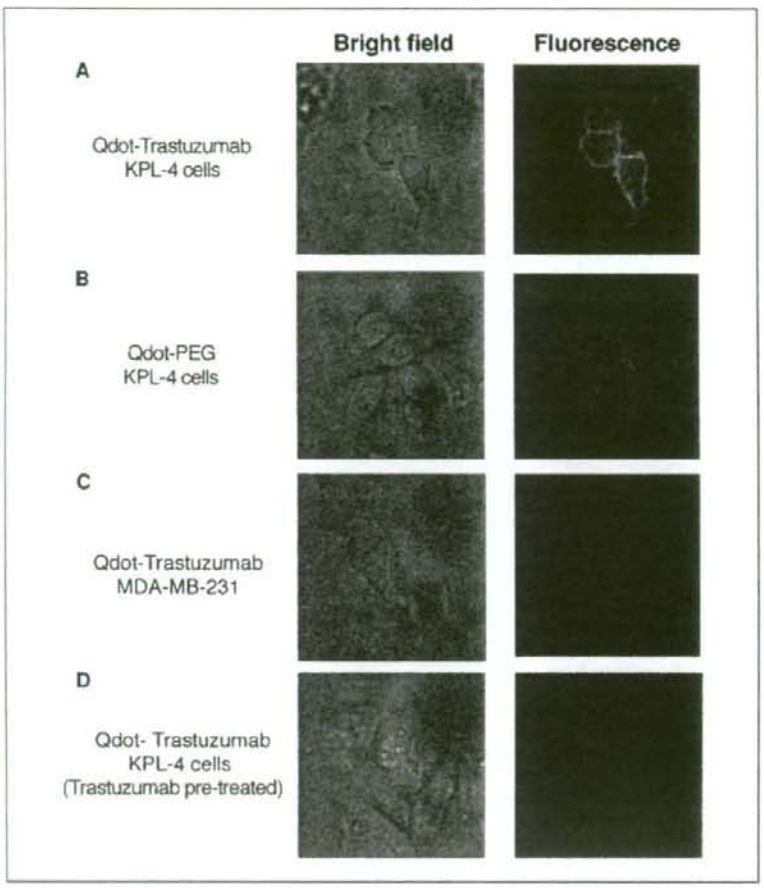

Figure 1. Immunocytochemical studies of QT-complex binding activity in cultured breast cancer cells. *A*, KPL-4 cells, which are HER2 positive, as revealed by the presence of the QT complex on the cell surface. *B*, negative staining was detected in KPL-4 cells exposed to QD-PEG in the absence of anti-HER2 antibody. *C*, negative staining was detected in MDA-MB-231 cells, which are HER2 negative. *D*, competition study of QT complex and trastuzumab. After addition of 100 nmol/L trastuzumab to KPL-4 cells, QT-complex fluorescence was absent. QT-complex fluorescence was detected on the cell surface of KPL-4 but not MDA-MB-231, confirming HER2 as a cell surface–specific marker for some breast cancer cell lines.

has been found to have little or no effect on their binding ability. QT complex [Qdot (Q)-trastuzumab (T) complex] was fractionated by agarose gel electrophoresis into three major bands. Approximately 60% of the QT complex was conjugated with three antibody fragments, ~30% with two fragments, and ~10% with a single fragment (data not shown).

The final concentration of QT complexes was determined by measuring the conjugate absorbance at 550 nm and using an extinction coefficient of 1,700,000 M^{-1} cm^{-1} at 550 nm.

Cell line and mouse model. The human breast cancer cell line KPL-4, which overexpresses HER2 and is sensitive to trastuzumab (15, 16), was kindly provided by Dr. J. Kurebayashi (Kawasaki Medical school, Kurashiki, Japan). KPL-4 cells were cultured in DMEM supplemented with 5% fetal bovine serum (FBS). MDA-MB-231 cells were maintained in RPMI with 10% FBS. Conventional immunohistochemical procedures were used to determine the binding of QT-complex conjugate to KPL-4 cells, using both QD-PEG (no antibody) and MDA-MB-231 as negative controls. In these studies, QT-complex or QD-PEG bioconjugates (100 nmol/L) were incubated with the cells for 30 min at 37°C, washed, and photographed. For competition study of QT complex and trastuzumab, KPL-4 was pretreated with trastuzumab (100 nmol/L) for 30 min before exposure to 100 nmol/L QT complex.

A suspension of KPL-4 cells (0.8×10^7 per mouse) was transplanted s.c. to the dorsal skin of female BALB/c *nu/nu* mice at 6 to 10 weeks of age (Charles River Japan, Yokohama, Japan). Several weeks after tumor inoculation, mice bearing a tumor volume of 100 to 200 mm^3 were selected. All of the mice were maintained in our pathogen-free institutional facilities. All operations on animals were in accordance with the institutional animal use and care regulations.

QT complexes were injected into the tail vein of mice at a concentration of 2 μmol/L and a volume of 100 μL. The mice were placed under anesthesia by the i.p. injection of a ketamine and xylazine mixture at dosages of 95 and 5 mg/kg, respectively. The temperature of mice was maintained at 37°C with a thermoplate and objective lens heater.

The dorsal skinfold chamber, previously described (13) and modified for this study, was used to fix the exposed mouse tumor on the stage of the microscope. Two sterilized polyvinyl chloride plates (0.5-mm thickness) containing a window were mounted to fix the extended double layer of dorsal skin including the tumor site. Skin between chambers was sutured together with 6-0 nylon around the window so the tumor could be located in the center of the window and fixed without influence from the beating of the heart and/or breathing. The tumor was exposed by oval incision of ~10-mm diameter, and the s.c. connective tissue was removed. The tumor was then placed surface down in neutral saline, mounted on coverslip, and viewed under an inverted microscope. The mouse was fixed to a metal plate on the stage designed to stabilize the chamber. Tumors can be visualized directly by means of this setup.

After imaging, the mice were sacrificed by CO_2 overdose. The tumors were removed and divided for histologic Qdot uptake study and immunohistochemical analysis. For the histologic Qdot uptake study, tumors were frozen and cryosectioned (6-mm thickness), fixed with acetone at 0°C, and examined with an imaging system. For immunohistologic examination, tumors were fixed in 10% neutral-buffered formalin overnight and then transferred to ethanol before processing and paraffin embedding. Immunohistochemical analysis was done on paraffin sections of 6-mm thickness using the HercepTest (DakoCytomation, Carpinteria, CA).

***In vivo* imaging and tracking.** *Optics and image analysis:* The optics system for three-dimensional observation consisted primarily of an epifluorescent microscope (IX71, Olympus, Tokyo, Japan) with modifications (17, 18), a Nipkow lens type confocal unit (CSU10, Yokokawa, Japan), and an electron multiplier type CCD camera (iXon 887, Andor, Tokyo, Japan). The confocal unit adopts multibeam scanning using about a thousand beams that are simultaneously emitted through a pin-hole disk to facilitate high-speed scanning. The EMCCD has an advantage that offers unsurpassed sensitivity performance and has been shown to yield markedly improved S/N (signal/noise) ratio (14). The object lens (60×, numerical aperture 1.45) was moved by a piezo actuator with a feedback loop (Nanocontrol) for stabilizing the position of the focus. A computer controlled the piezo actuator in synchronization with the image acquisitions that the object lens remained within the exposure time of the CCD camera. An area of ~ 30 × 30 μm^2 was illuminated by a green laser (532 nm, CrystaLaser, Reno, NV). This system captures images of single Qdot at a video rate of 33 ms/frame. Three-dimensional confocal intravital images of single QT complex were taken by moving an objective lens (Fig. 2*A*). Three-dimensional images of the tumor were taken by reconstructing 10 to 20 confocal images from the surface of the mice to a depth of 150 μm inside the tumor through the DSCF.

The *xy* position of the fluorescent spot was calculated by fitting to a two-dimensional Gaussian curve. The single molecule could be identified by the fluorescence intensity. In addition, quantitative and qualitative information such as velocity, directionality, and transport mode was obtained using time-resolved trajectories of particles. The resolution of the position was determined from the position of immobile QT complexes in a chemically fixed tumor cell. The resolution of the *x* and *y* directions of images taken at an exposure time of 33 ms was 30 nm, taking into consideration the SD.

Results and Discussions

***In vitro* study.** Qdots were conjugated to trastuzumab using the Qdot-antibody conjugation kit (QT complex). Immunocytochemical data confirmed strong and specific binding of the QT complex to a HER2-overexpressing human breast cancer cell line (Fig. 1*A*). QD-PEG without antibody showed almost no binding to KPL-4 cells (Fig. 1*B*). MDA-MB-231, a HER2 negative human breast cancer cell line, showed the absence of Qdot binding (Fig. 1*C*). KPL-4 cells pretreated by excess trastuzumab also showed the absence of Qdot binding (Fig. 1*D*). These results indicate that QT complexes selectively bind to the HER2 protein. Furthermore, QT complex was compared with trastuzumab labeled with rhodamine, which is recognized as similar to native trastuzumab. Both QT complex and rhodamine-trastuzumab bound to the KPL-4 cell at concentrations of 1 nmol/L but hardly at 0.1 nmol/L, indicating the binding properties of QT complex are similar to those of native antibody (data not shown).

Three-dimensional imaging of single Qdot-trastuzumab in mice. It is reported that the accumulation of trastuzumab at the HER2-overexpressing tumor site in mice model is the basis for radioimmunoscintigraphic scanning and targeted therapy for human HER2-overexpressing breast cancer (19–21). Here tumor-bearing mouse models were prepared with KPL-4 s.c. implantation. The QT complex accumulated in the tumor specifically because only the tumor area generated fluorescence of Qdots (Supplementary Fig. S1*A* and *B*). Single Qdots in the mice tumor were observed using a high-resolution intravital imaging system through the dorsal skinfold chamber (Fig. 2*A*; ref. 13). Fluorescence microangiography was done after injection of the QT complexes into the tail vein. After injection, blood sample from mice was examined by fluorescence observation on whether QT complex had made the aggregation in the mice. QT complex existed as a single particle without further aggregation (data not shown). The membranes of the KPL-4 tumor cells were clearly stained with single QT complexes at 6 h after the injection. At 24 h after the injection, the QT complexes had been internalized into the tumor cells (Fig. 2*B* and *C*). After imaging of the tumors in the living mice, histologic examination of the chemically fixed tumors was done to confirm that QT complexes in the living mice exhibit activity in KPL-4 cells. QT complexes observed under a three-dimensional microscope were located at the cell membrane and near the nuclear membrane (Supplementary Fig. S2*A* and *B*). An adjacent slice of the observed area was further stained

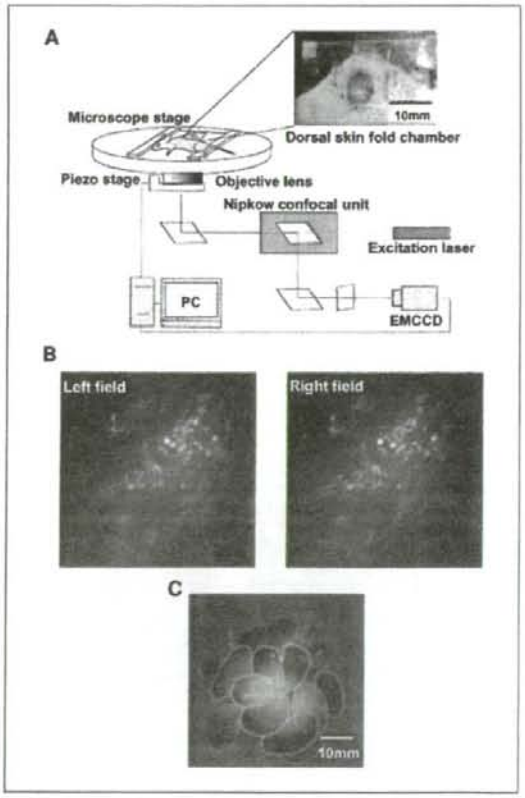

Figure 2. Experimental diagram and three-dimensional intravital cancer imaging. Mice prepared for dorsal skinfold chamber were fixed on the microscopic stage. QT complexes were injected into the tail vein of nude BALB/c mice bearing KPL-4 breast cancer xenograft tumor. *A*, three-dimensional microscopic system consisting of a confocal unit, an EMCCD, and a computer to control the piezo stage. *B*, three-dimensional image of the tumor was obtained by the QT complexes binding to tumor cell membrane (stereoscopic image: left and right field). *C*, traced outlines of the cells shown in (*B*).

immunohistochemically with the anti-HER2 antibody A0485. The cell membrane stained locally in the adjacent slice (Supplementary Fig. S2C), confirming that QT complexes were present on the membrane of tumor cells.

Extravasation of single QT complexes in tumors of mice with two-dimensional imaging. After the injection, three-dimensional images of the tumor were taken to allow observation on the tumor vessel of single QT complexes. The position of the objective was fixed and 300 to 3,000 sequential confocal two-dimensional images (total, 10–100 s) were taken at this fixed position. Within 30 s after the injection, the current of the QT complex in a vessel was observed. When the vessel and cells were clearly observable, the the current of single QT complex in the tumor vessel was then analyzed. The fluorescent image of the circulating QT complex was not a circle but an ellipse and sometimes a line at the video rate because QT complex at times moved >1 μm in single frame. The speed of the movement of the single particles was calculated from the positional changes of the centroid of the QT complex images (Fig. 3A). The average speed of each complex ranged from 100 to 600 μm/s, in agreement with a previous report by another method (22). As shown in Fig. 3A, each particle exhibits slow and fast movement in the bloodstream. Such fast and slow movement characteristics could be induced by the pulse and nonuniform current within a vessel such as the Hagen-Poiseuille current. The slow speed of the complexes inside a tumor vessel would be important to locate pores between the vessel cells and then the complexes diffuse out from these pores. F3

Focusing on the vessel walls, a movement was observed of the complex extravasated from the intravascular space (Fig. 3B). The edge of the vascular inner surface was not clear on a single frame image. Therefore, all the images obtained were averaged to precisely determine the position of the edge (Fig. 3B, *i–iii*). The complexes were positioned first on the vascular surface and then extravasated. This is the first example of video rate observation of extravasation of very small particles, such as Qdots, in a mouse model. The moving speed of the complexes was very low, 1 to 4 μm/s, at the pore of the vascular cells, compared with the speed in the current. The QT complexes either interacted with the vascular cells or became trapped in the extracellular matrix.

Diffusion of single QT complexes in extracellular and intercellular regions. Two hours after the injection, many complexes had migrated into the tumor interstitial area close to the tumor vessels. Most of the movement of the complexes was random in orientation and speed, indicating that complexes diffuse by the Brownian motion exerted by thermal energy. The average diffusion coefficient of the complexes was 0.0014 $\mu m^2/s$, much smaller than that at free diffusion in solution ($\sim 10\ \mu m^2/s$). Many complexes also moved randomly within a restricted small area of ~1-μm diameter and then hopped by ~1 μm (Fig. 4A). These results indicate that movement is restricted by a cage formed by the extracellular matrix and, at times, complexes escape from this cage. F4

Binding of QT complexes to cell membrane and vesicle transport. Six hours after the injection, QT complexes had bound to the KPL-4 cell membrane on which the HER2 protein is located. We successfully captured specific images of the QT complexes bound to the cell membrane (Fig. 4B). Movements of single QT complex are identified in single frames. To identify the positions of the tumor vessels and cells in living mice without further fluorescence staining, images were averaged (Supplementary Fig. S3A). As viewed from the outside of the delineated cells, the QT complexes moved toward the cell membrane at a speed of 200 to 400 nm/s (Fig. 4C), remained on the membrane for a few seconds, and then moved randomly along the membrane. QT complexes moved between the cells, bound to HER2, and then moved in association with HER2 on the membrane. SF3

Many QT complexes bound to the cell membrane exhibited Brownian motion within a restricted region of ~500-nm diameter. The region is significantly larger than the area of ~30 nm, which was drawn by position noise of the complexes fixed on a coverslip, indicating the movement is due to the anchor of the HER2 to a flexible component of the cytoskeleton such as an actin filament (23). The QT complexes restricted to the small area initiated linear movement in one direction along the cell membrane with a speed of 400 to 600 nm/s and traveled for several micrometers (Fig. 5A and B; Supplementary Fig. S3B). F5

We also succeeded in pursuing the transport of QT complexes from the peripheral region of the cell to the perinuclear region

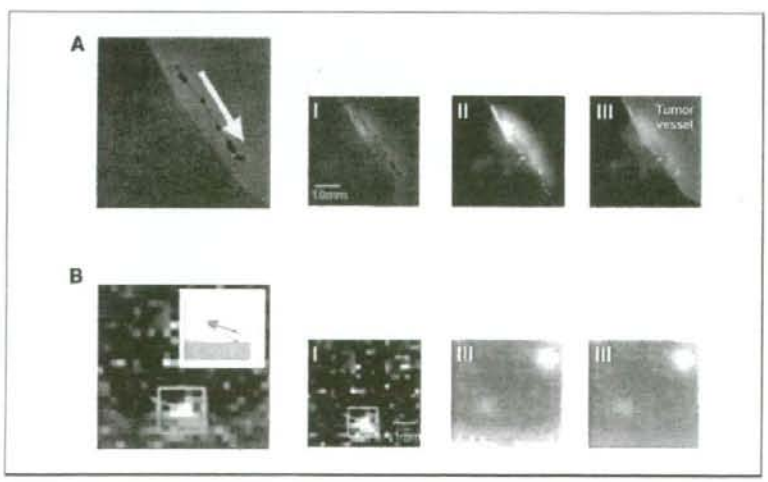

Q8

Figure 3. The movement of QT complexes from tumor vessels to the interstitial space. *A*, flow of QT complexes in the tumor vessel. The speed was calculated by the moving distance per 33 ms. The maximum speed was ~600 μm/s. *B*, extravasation of QT complexes from the vascular space of the tumor. *Dotted line*, trajectory of the extravasation. *i*, an initial single frame tracing the trajectory of a single QT complex shown as a dotted line at video rate. *ii*, sequential frames were averaged to define the edge of vessel. *iii*, tracing of the outlines of tumor vessels. Overlapping initial single image and (*iii*), the tracing image gives the final images. *B*, *inset*, magnified image of the trajectory of extravasating QT complex.

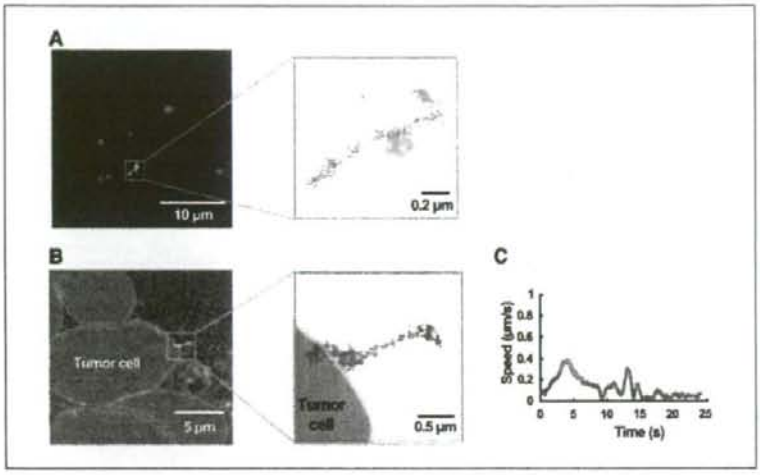

Figure 4. Tracking the movement of QT complexes from the interstitial space to the cell membrane. *A*, trajectory of the QT complexes in the interstitial space near the tumor vessels and magnified trajectory. The color of the trajectory codes the time axis from black to pink, yellow, and light blue. *B*, trajectory of the binding to the cell membrane and magnified trajectory. *C*, time trajectory of the velocity of (*B*). The color of the trajectory of both (*B*) and (*C*) codes the time axis from blue to red and green. All time trajectories of the velocity are calculated by the least squares method (2 s).

(Fig. 5*C*; Supplementary Fig. S3*C*). The QT complex in a given cell moved almost straight toward the cell membrane with a velocity of 100 to 300 nm/s, changed direction to parallel to the cell membrane, and moved toward the cell nucleus at a velocity of ~600 nm/s (Fig. 5*D*). Finally, the directional movement of the QT complexes ceased and Brownian motion commenced within a small area, ~1 μm in a diameter, near the nucleus (Fig. 5*C* and *D*, *black line*). The first two movements of straight toward and along the cell membrane would most likely be produced by the transport of an acto-myosin system binding to vesicle containing QT complexes (24, 25). Because the actin filaments in cultured cells are highly concentrated in the peripheral region of cells, movement toward the nucleus would most likely be on a microtubule transported by dynein (26) as there are almost no actin filaments near nucleus, but rather, a high concentration of microtubules.

Summary of the delivery processes. We have succeeded in capturing the specific delivery of single QT complexes in tumor vessels to the perinuclear region of tumor cells in live mice after QT complexes had been injected into the tail vein of mice. Six stages were detected (Fig. 6): (*a*) vessel circulation, (*b*) extravasation, (*c*) movement into the extracellular region, (*d*) binding to HER2 on the cell membrane, (*e*) movement from the cell membrane to the perinuclear region after endocytosis, and (*f*) in the perinuclear region. The translational speed of QT complexes in each process was highly variable, even in the vessel circulation. The movement of the complexes in each process was also found to be "stop-and-go" (i.e., the complex remaining within a highly restricted area and then moving suddenly). This indicates that the movement was promoted by a motive power and constrained by both the three-dimensional structure and protein-protein interactions. The motive

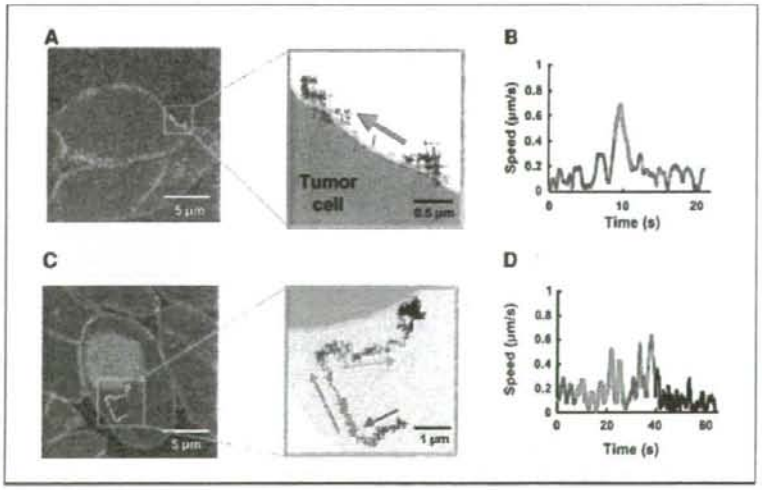

Figure 5. Tracking of the movement of QT complexes from the cell membrane to the perinuclear region. *A*, trajectory of the QT complexes binding to the cell membrane and magnified image. *B*, time trajectory of the velocity of (*A*). The color of the trajectory of both (*A*) and (*B*) codes the time axis from blue to red and green. *C*, trajectory of the intracellular transport of QT complex and magnified image. *D*, time trajectory of the velocity of (*C*). The color of the trajectory of both (*C*) and (*D*) codes the time axis from blue to red, green, and black. All time trajectories of the velocity are calculated by the least squares method (2 s).

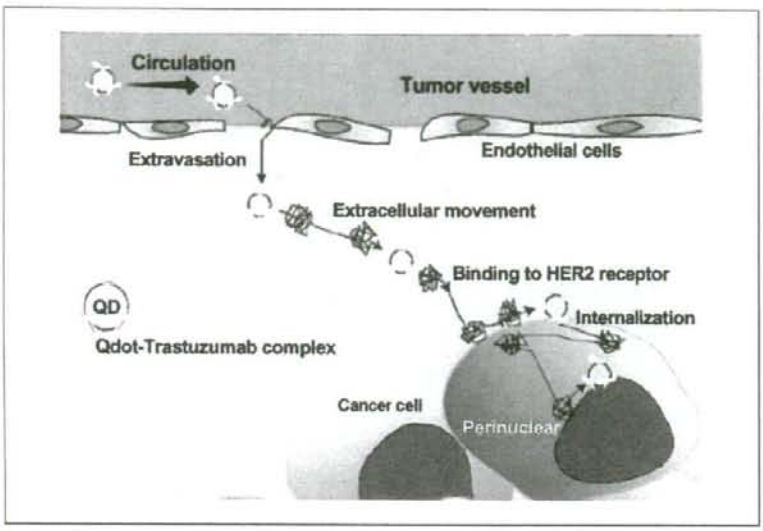

Q8

Figure 6. Schematic illustration of the QT complex, the QT complex entered into the circulation, extravasated into the interstitial space from the vascular space, bound to the tumor cells through the interstitial region, and having reached the perinuclear region after traveling on the intracellular rail protein. All processes exhibit a characteristic stop-and-go movement.

power of the movements was produced by blood circulation (essential in processes *a* and *b*), diffusion force driven by thermal energy (*b*, *c*, and *d*), and active transport by motor proteins (*e*). The cessation of movement is most likely induced by a structural barricade such as a matrix cage (*b*, *c*, and *f*) and/or specific interaction between proteins (e.g., an antibody) and HER2 (*d*), motor proteins, and rail filaments such as actin filaments and microtubules (*e*).

The molecular mechanism underlying the movement and its cessation during delivery of nanoparticles in animal models is the fundamental basis of drug delivery. There have been many different approaches to tumor-targeting "nanocarriers" including anticancer drugs for passive targeting, such as Myocet (27) and Doxil (28), and for active targeting, such as MCC-465 (29) and anti-HER2 immunoliposome (19). There is still very little understanding of the biological behavior of nanocarriers, including such crucial features as their transport in the blood circulation, cellular recognition, translocation into the cytoplasm, and final fate in the target cell. These results suggest that the transport of nanocarriers would be quantitatively analyzable in the tumors of living animals by the present method. This approach should thus afford a potential new insight into particle behavior in complex biological environments. Such new insight in turn will allow rational improvements in particle design to increase the therapeutic index of the tumor-targeting nanocarriers.

Acknowledgments

Received 4/4/2006; revised 8/24/2006; accepted 12/5/2006.

Grant support: Grants-in-aid for Research Project; Promotion of Advanced Medical Technology (H14-Nano-010); Ministry of Health, Labor, and Welfare of Japan (N. Ohuchi); Scientific Research in Priority Areas from the Japan MEXT (H. Higuchi); and Special Coordination Funds for Promoting Science and Technology of Japan (H. Higuchi, T.M. Wanatabe, and N. Ohuchi).

The costs of publication of this article were defrayed in part by the payment of page charges. This article must therefore be hereby marked *advertisement* in accordance with 18 U.S.C. Section 1734 solely to indicate this fact.

We thank Dr. H.A. Nguyen for helpful discussion and Dr. J.M. West for critical reading of the manuscript.

References

1. Mamot C, Drummond DC, Noble CO, et al. Epidermal growth factor receptor-targeted immunoliposomes significantly enhance the efficacy of multiple anticancer drugs *in vivo*. Cancer Res 2005;65:11631–8.
2. Torchilin VP, Lukyanov AN, Gao Z, Papahadjopoulos-Sternberg B. Immunomicelles: targeted pharmaceutical carriers for poorly soluble drugs. Proc Natl Acad Sci U S A 2003;100:6039–44.
3. Krauss WC, Park JW, Kirpotin DB, Hong K, Benz CC. Emerging antibody-based HER2 (ErbB-2/neu) therapeutics. Breast Dis 2000;11:113–24.
4. Ishijima A, Kojima H, Funatsu T, et al. Simultaneous observation of individual ATPase and mechanical events by a single myosin molecule during interaction with actin. Cell 1998;92:161–71.
5. Lyons SK. Advances in imaging mouse tumour models *in vivo*. J Pathol 2005;205:194–205.
6. Wu X, Liu H, Liu J, et al. Immunofluorescent labeling of cancer marker Her2 and other cellular targets with semiconductor quantum dots. Nat Biotechnol 2003;21:41–6.
7. Bruchez M, Jr., Moronne M, Gin P, Weiss S, Alivisatos AP. Semiconductor nanocrystals as fluorescent biological labels. Science 1998;281:2013–6.
8. Gao X, Cui Y, Levenson RM, Chung LW, Nie S. *In vivo* cancer targeting and imaging with semiconductor quantum dots. Nat Biotechnol 2004;22:969–76.
9. Endow SA, Higuchi H. A mutant of the motor protein kinesin that moves in both directions on microtubules. Nature 2000;406:913–6.
10. Yildiz A, Forkey JN, McKinney SA, Ha T, Goldman YE, Selvin PR. Myosin V walks hand-over-hand: single fluorophore imaging with 1.5-nm localization. Science 2003;300:2061–5.
11. Dahan M, Levi S, Luccardini C, Rostaing P, Riveau B, Triller A. Diffusion dynamics of glycine receptors revealed by single-quantum dot tracking. Science 2003;302:442–5.
12. Lidke DS, Nagy P, Heintzmann R, et al. Quantum dot ligands provide new insights into erbB/HER receptor-mediated signal transduction. Nat Biotechnol 2004;22:198–203.
13. Leunig M, Yuan F, Menger MD, et al. Angiogenesis, microvascular architecture, microhemodynamics, and interstitial fluid pressure during early growth of human adenocarcinoma LS174T in SCID mice. Cancer Res 1992;52:6553–60.
14. Chong FK, Coates CG, Denvir DJ, McHale NG, Thornbury KD, Hollywood MK. Optimization of spinning disk confocal microscopy: synchronization with the ultra-sensitive EMCCD. Proc SPIE 2004;5324:65–76.
15. Kurebayashi J, Otsuki T, Tang CK, et al. Isolation and characterization of a new human breast cancer cell line, KPL-4, expressing the Erb B family receptors and interleukin-6. Br J Cancer 1999;79:707–17.

16. Fujimoto-Ouchi K, Sekiguchi F, Tanaka Y. Antitumor activity of combinations of anti-HER-2 antibody trastuzumab and oral fluoropyrimidines capecitabine/5′ dFUrd in human breast cancer models. Cancer Chemother Pharmacol 2002;49:211–6.
17. Nguyen VT, Kamio Y, Higuchi H. Single-molecule imaging of cooperative assembly of γ-hemolysin on erythrocyte membranes. EMBO J 2003;22:4968–79.
18. Nguyen H, Higuchi H. Motility of myosin V regulated by the dissociation of single calmodulin. Nat Struct Mol Biol 2005;12:127–32.
19. Park JW, Kirpotin DB, Hong K, et al. Tumor targeting using anti-her2 immunoliposomes. J Control Release 2001;74:95–113.
20. Ballangrud AM, Yang WH, Palm S, et al. α-Particle emitting atomic generator (Actinium-225)-labeled trastuzumab (Herceptin) targeting of breast cancer spheroids: efficacy versus HER2/neu expression. Clin Cancer Res 2004;10:4489–97.
21. Wiercioch R, Balcerczak E, Byszewska E, Mirowski M. Uptake of radiolabelled Herceptin by experimental mammary adenocarcinoma. Nucl Med Rev Cent East Eur 2003;6:99–103.
22. Braun RD, Abbas A, Bukhari SO, Wilson W III. Hemodynamic parameters in blood vessels in choroidal melanoma xenografts and rat choroid. Invest Ophthalmol Vis Sci 2002;43:3045–52.
23. Carraway CA, Carvajal ME, Carraway KL. Association of the Ras to mitogen-activated protein kinase signal transduction pathway with microfilaments: Evidence for a p185(neu)-containing cell surface signal transduction particle linking the mitogenic pathway to a membrane-microfilament association site. J Biol Chem 1999;274:25659–67.
24. Buss F, Arden SD, Lindsay M, Luzio JP, Kendrick-Jones J. Myosin VI isoform localized to clathrin-coated vesicles with a role in clathrin-mediated endocytosis. EMBO J 2001;20:3676–84.
25. Aschenbrenner L, Naccache SN, Hasson T. Uncoated endocytic vesicles require the unconventional myosin, Myo6, for rapid transport through actin barriers. Mol Biol Cell 2004;15:2253–63.
26. Kamal A, Goldstein LS. Connecting vesicle transport to the cytoskeleton. Curr Opin Cell Biol 2000;12:503–8.
27. Mross K, Niemann B, Massing U, et al. Pharmacokinetics of liposomal doxorubicin (TLC-D99; Myocet) in patients with solid tumors: an open-label, single-dose study. Cancer Chemother Pharmacol 2004;54:514–24.
28. O'Brien ME, Wigler N, Inbar M, et al. Reduced cardiotoxicity and comparable efficacy in a phase III trial of pegylated liposomal doxorubicin HCl (CAELYX/Doxil) versus conventional doxorubicin for first-line treatment of metastatic breast cancer. Ann Oncol 2004;15:440–9.
29. Hamaguchi T, Matsumura Y, Nakanishi Y, et al. Antitumor effect of MCC-465, pegylated liposomal doxorubicin tagged with newly developed monoclonal antibody GAH, in colorectal cancer xenografts. Cancer Sci 2004;95:608–13.